Thermal and Mechanical Behaviour of a Subassembly Hexcan Under Total Instantaneous Blockage Conditions; A Code Comparison

R. O. Attinger, W. Heer, P. Wydler
Paul Scherrer Institute, Villigen PSI, Switzerland
D. Desprez, J. Louvet
CEA–CEN Cadarache, St. Paul–lez–Durance, France
A. Zucchini
ENEA, CRI E. Clemetel, Bologna, Italy

INTRODUCTION

The total instantaneous blockage (TIB) of a subassembly at nominal power plays an important role in the safety philosophy of future fast reactors. In the thermal melt–propagation scenario of the TIB, a central question concerns the mode of failure of the subassembly wrapper. To provide a basis for validating data and methods used in the thermal and mechanical analysis of the behaviour of the wrapper, CEA–DRP at Cadarache is carrying out the COTHAA experiments (Desprez et al., 1989), in which circular and hexagonal tubes are heated and pressurized to failure under controlled conditions. In this context three calculational benchmarks have been formulated and analysed using the heat transfer codes DELFINE (CEA) and ADINAT (PSI) in combination with the stress analysis codes INCA (CEA), SOLVIA (PSI) and ABAQUS (ENEA).

The aim of the first benchmark problem was to validate the heat transfer codes against a simple problem for which there exists an analytical solution. In this exercise emphasis was on the treatment of the latent heat. The second benchmark problem dealt with the heat conduction in a hexagonal wrapper (hexcan) subjected to TIB thermal loads. The mechanical response of the wrapper was determined in the third benchmark problem using a decoupled thermomechanical theory. This benchmark exercise allowed to compare the methods for treating weakening of materials near the melting point and to investigate the influence of geometric nonlinearities.

HEAT CONDUCTION IN A SEMI–INFINITE REGION

A one–dimensional heat conduction problem with melting is calculated: A semi–infinite region has an initial temperature which is constant over the whole space, suddenly a temperature larger than the melting temperature is maintained at the free surface. The resulting temperature transients are determined using the DELFINE and ADINAT codes with one– and two–dimensional meshes; the latter was used for verification purposes. Constant but different material properties were taken for the solid and the liquid phases. The numerical results are compared to the exact analytical solution given by Carslaw and Jaeger, 1959. For the melt front $\tilde{x}(t)$ the analytical expression is

$$\tilde{x}(t) = 2\Lambda \cdot \sqrt{\alpha_l \cdot t}.$$

The dimensionless melting constant Λ and the thermal diffusivity of the liquid region α_l are 0.301 and 3.319 mm^2/s, respectively.

Two methods for modelling the melting process are considered in the finite element codes. These involve a melting model based on the enthalpy method (Rolph and Bathe, 1982) and an equivalent variation of the heat capacity, the so–called c–variation model. In the ADINAT code, the melting model is restricted to a lumped approximation for the specific heat capacity and to the Euler backward time integration; the melting model in the DELFINE code and the c–variation model require no such limitations.

In general, the numerical and the analytical results agree quite well. Figure 1 shows the position of the melt front $\tilde{x}(t)$ calculated with two–dimensional meshes. Both the melting and the c–variation model give a good representation of the melting phenomenon, provided the spatial mesh and the time steps are chosen appropriately. In combination with a fine spatial mesh the melting model can accomodate larger temperature increments per time step or element size than the c–variation model. The melting model of DELFINE appears to model the passage of the melt–front through element boundaries more accurately than the melting model of ADINAT; whereas ADINAT still converges in cases where DELFINE fails because of too large temperature increments. With the c–variation model, the time step has to be sufficiently small to ensure an adequate sampling of the effective specific heat capacity near the melting temperature. Some inaccuracies are observed at the beginning of the calculation. They are caused by the infinite temperature gradient at the hot boundary; therefore, the calculations were started from the analytical solution at times as indicated in the table of Figure 1. The infinite temperature gradient is particular to this benchmark problem.

TEMPERATURE EVOLUTION IN A HEXCAN

The temperature evolution is determined in a subassembly wrapper of the form of a Superphénix hexcan. The heat flux at the inner surface of the hexcan, the heat exchange to the surrounding sodium and the temperature of the sodium are given (Figure 2). The resulting temperature transients are calculated using the DELFINE and ADINAT codes with a two–dimensional mesh and material properties as given in Figure 3.

Figure 4 shows the calculated temperature evolution in the midst of the face of the hexcan. Up to the onset of melting at around 22 s, the variations of the temperature reflect the variation of the heat flux at the inner surface and the temperature of the sodium at the outer surface. The onset of melting has a small effect on the rate of temperature increase at the inner surface. At 27 s, the heat exchange to the surrounding sodium is interrupted, simulating evaporation of the sodium. In response, the temperature at the outer surface rapidly approaches the melting temperature, the ADINAT code predicting a nearly 1 s long plateau before complete melting is achieved. Upon melt–through, the disappearence of the mitigating latent heat effect further enhances the rate of temperature increase.

On the whole, the DELFINE and ADINAT predictions of the hexcan temperature evolution are in close agreement. Numerical instabilities at the onset of melting were encountered due to too large changes of the material properties per time step; they can be overcome by reducing the time steps. It could be shown that the c–variation model for the latent heat is applicable. Furthermore, it was confirmed that, for both codes, the range of convergence extends to beyond the point of complete melting of the hexcan.

STRUCTURAL RESPONSE OF THE HEXCAN

The aim of the third benchmark was to determine the structural response of a Superphénix hexcan under thermal load taken from the second benchmark and a superimposed pressure load. A further aim was to see how the numerical problems caused by loss of mechanical strength near the melting temperature are solved.

A thermoelastic–plastic bilinear material law and material properties according to Figure 3 were used in the finite element analyses. A plane strain state, the von Mises yield condition and isotropic hardening were assumed. The loss of mechanical strength near the melting temperature caused no numerical problems in the ABAQUS code. The convergence problems are overcome in the INCA code by setting temperatures above a certain cut–off temperature to this temperature. Inactive elements are used in the SOLVIA code for the simulation of the molten material and the radial return method was implemented in a user supplied material model for assuring convergence at high temperatures. The time steps in the INCA calculation were chosen to be constant, those in the SOLVIA calculation were chosen to produce temperature increments of about 50 °C, whereas the ABAQUS code adjusted the time steps automatically in the final part of the calculation. Basically, a small strain and small displacement formulation was used, but geometric nonlinearities were also considered in a complementary calculation using the large displacement formulation in the ABAQUS code.

The calculated midface and corner displacements are shown in Figure 5. The midface displacement clearly reflects the effect of the internal pressure ramp as given in Figure 2. The influence of the modelling of the molten material in the codes is small, the INCA and SOLVIA codes predicting a slightly stiffer behaviour of the structure than the ABAQUS code with the corresponding formulation. With the large displacement formulation, the ABAQUS code allows to model the temporary inward motion of the corner when – under the internal pressure – the hexcan tends to approach the more resistant geometry of a cylinder (Figure 7).

A useful quantity for predicting collapse of the hexcan is the ratio of the effective strain to the temperature dependent ultimate strain. The evolution of this ratio is shown in Figure 6 (it has to be taken into account that the results from the INCA code refer directly to the nodes while the results from the other two codes refer to the integration points). An interesting feature of the thermomechanical hexcan problem is that the strain ratio at the inner surface of the hexcan reaches a maximum after 12 s to 15 s and then becomes rather small when, in response to the temperature increase, the ultimate strain starts to increase more rapidly than the effective strain. At the outer surface of the hexcan, the large displacement formulation predicts a similar strain ratio behaviour with the difference that due to the slower outside temperature rise the maximum is reached only about 2 s before melt–through. The largest strain ratios are observed in the midst of the outer surface (point A in Figure 6). For the small displacement case, the analyses indicate collapse at around 25 s due to rapidly increasing strains. The large displacement calculation predicts the hexcan to collapse at 27.5 s through a uniform swelling. This time of collapse has been confirmed by an analytical analysis in one–dimensional ring geometry.

Up to nearly 24 s, corresponding to about 2 % strain and 3 mm to 4 mm maximum hexcan displacement, the INCA, SOLVIA and ABAQUS predictions of the important parameters are found to be in good agreement. In particular, there is good agreement for the maximum of the strain–ratio at the inner surface. A large displacement formulation seems to be necessary for modelling the phenomena in the last phase just before melt–through.

CONCLUSIONS

- The predictions of the temperature evolution and the mechanical response agree well.
- In the temperature analyses the effect of the latent heat may be simulated by a variation of the specific heat capacity. Numerical problems can be circumvented by an appropriate choice of the mesh and small time steps.
- In the mechanical analyses the method of modelling the molten material has a small influence on the results. The small displacement calculations agree with the large displacement calculation provided the strains do not exceed about 2 %.
- Geometric nonlinearities have to be considered for reliable solutions up to collapse.

REFERENCES

Carslaw, H.S., Jaeger, J.C.: "Conduction of Heat in Solids", Clarendon Press, Oxford, 2nd Ed. (1959), pp. 282–296.

Desprez, D., Louvet, J., Hamonet, P., Anziou, P.: "COTHAA Programme: An Experimental Approach to Thermomechanical Aspects of the TIB of a Subassembly", 10th SMiRT, Anaheim (Cal., USA), 1989, Division E.

Rolph, W.D. III, Bathe, K.J.: "An Efficient Algorithm for Analysis of Nonlinear Heat Transfer With Phase Changes", Int. J. Num. Meth. Engng., **18** (1982), pp. 119–134.

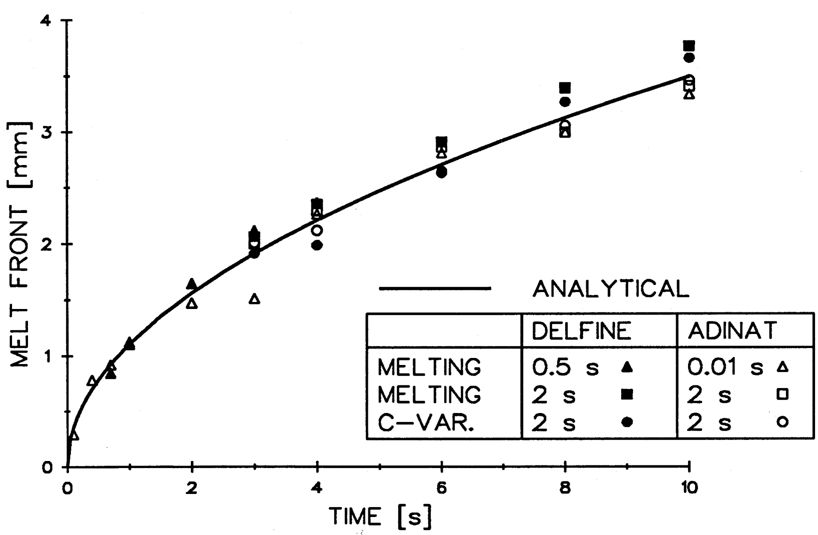

Figure 1: Propagation of the melt front in a semi-infinite region.

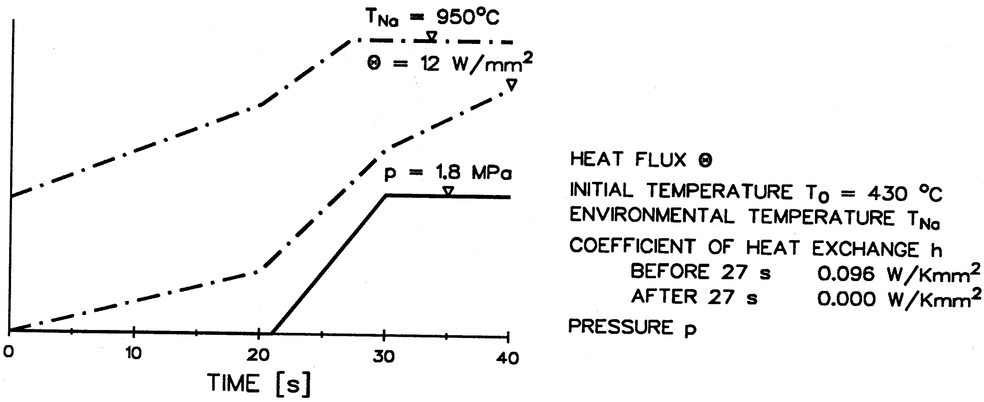

Figure 2: Loading conditions.

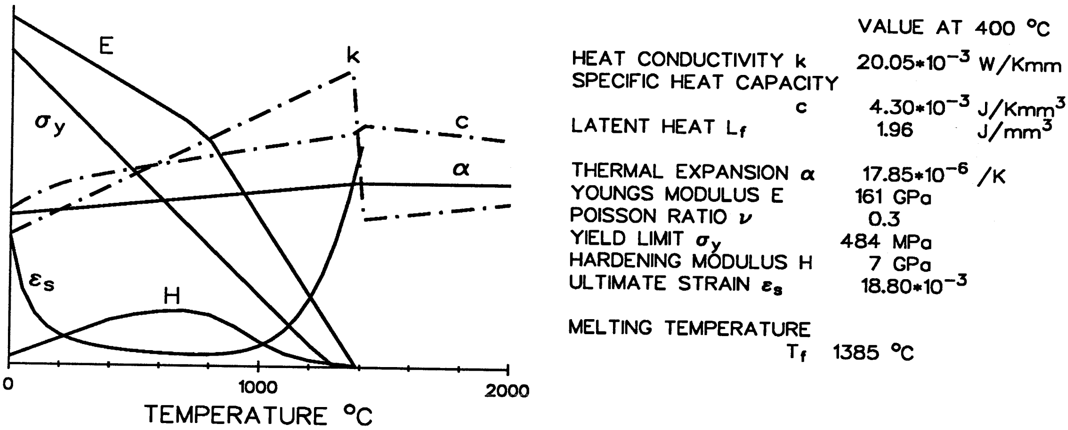

Figure 3: Material properties.

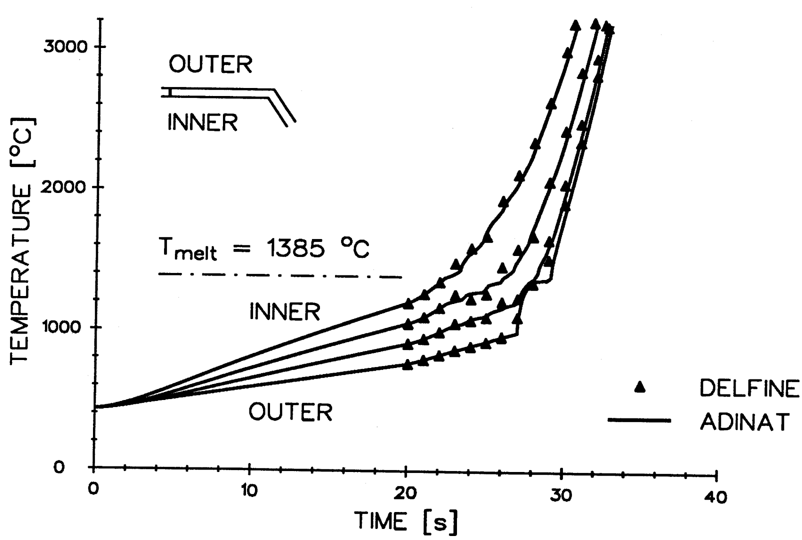

Figure 4: Temperature evolution in the hexcan.

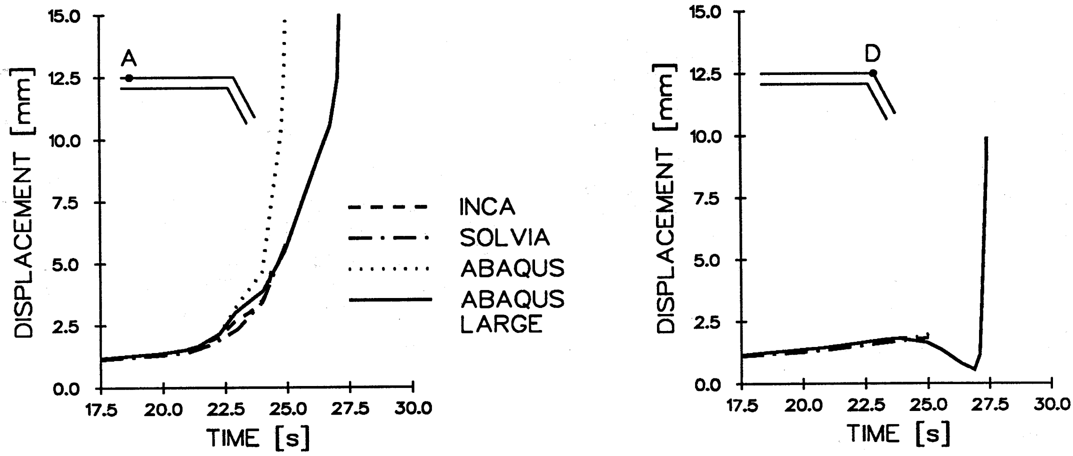

Figure 5: Displacement in the hexcan.

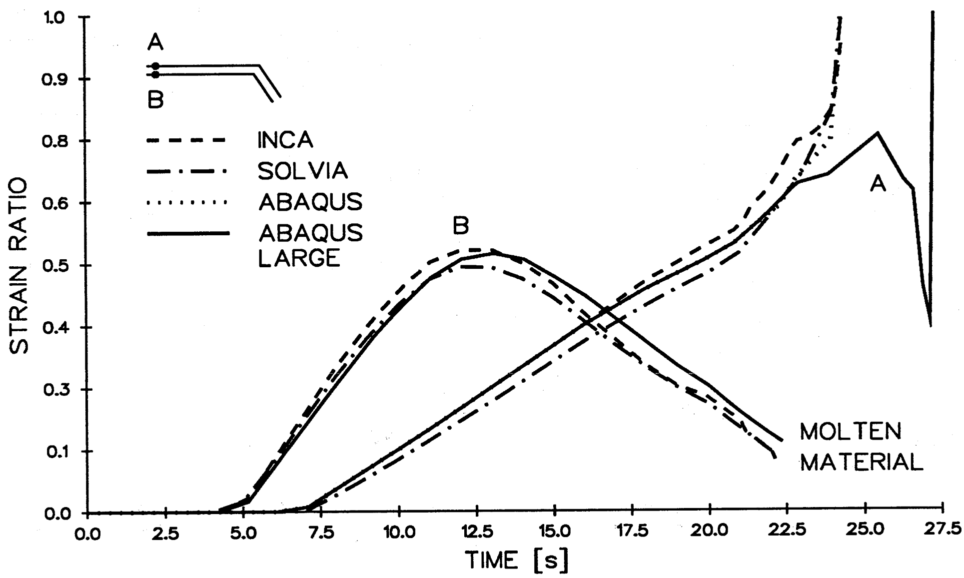

Figure 6: Strain ratio to determine collapse at midface.

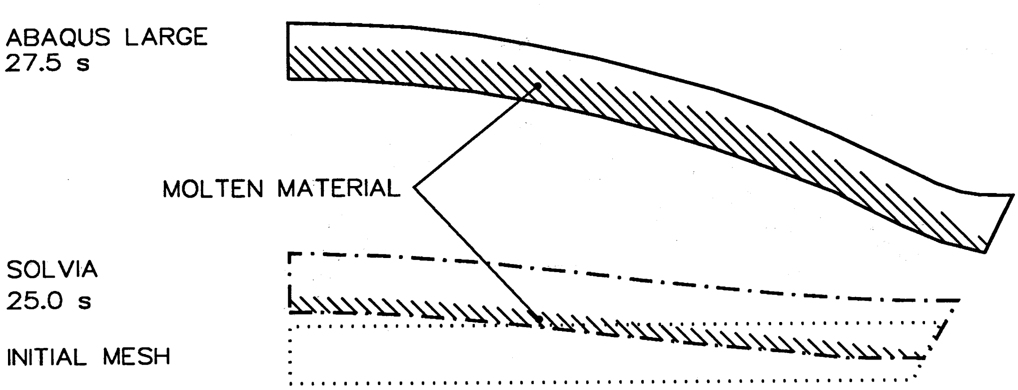

Figure 7: Deformed hexcan at collapse.